BRIDGES BETWEEN GEOMETRY AND GRAPH THEORY

Tomaž Pisanski   Milan Randić

Bridges between Geometry and Graph Theory

Tomaž Pisanski[*]

Tomaz.Pisanski@fmf.uni-lj.si

Institute of Mathematics, Physics and Mechanics
Department of Theoretical Computer Science
and
University of Ljubljana,
Department of Mathematics
Ljubljana, Slovenia

Milan Randić

Department of Mathematics and Computer Science
Drake University, Des Moines, Iowa

Abstract

Graph theory owes many powerful ideas and con-
structions to geometry. Several well-known families
of graphs arise as intersection graphs of certain ge-
ometric objects. Skeleta of polyhedra are natural
sources of graphs. Operations on polyhedra and
maps give rise to various interesting graphs. An-
other source of graphs are geometric configurations
where the relation of incidence determines the adja-
cency in the graph. Interesting graphs possess some
inner structure which allows them to be described
by labeling smaller graphs. The notion of covering
graphs is explored.

1 Introduction

We assume that the reader is familiar with basic
mathematics. For instance, we will not give any
geometric introduction. We expect that the reader
is familiar with concepts such as group, graph, ma-
trix, and permutation, but we do not require any
advanced knowledge of any of these topics. We do
not give any rigorous definition of surface or map
on a surface.

Books listed among our references, [5, 6, 7, 8, 11,
13, 14, 15, 18, 28, 29, 31, 32, 35, 37, 59, 66, 67, 68]
provide a spectrum of bacground material spanned
between motivating and introductory chapters for
general readership and ranging up to advanced and
rigorous monographs that can be used as a follow-
up to those readers who would really like to special-
ize their knowledge in a particular theme that we
touch here.

2 Intersection Graphs

Given a set of n points $V = \{v_1, v_2, \ldots, v_n\}$ in some
metric space and a positive number $r > 0$, we may
draw n closed balls $B_i := B(v_i, r), i = 1, 2, \ldots, n$,
each ball B_i centered at v_i and having radius r.
Define a graph $G(V, r)$ as follows: The vertices are
the n selected points. Two vertices v_i and v_j are
adjacent iff the corresponding balls intersect, i.e. if
$B_i \cap B_j \neq \emptyset$. The radius r will be called a *unit* and
the graph the *unit sphere graph*.

We will use the notation 2D to represent the stan-
dard Euclidean plane and 3D to represent Euclidean
3-dimensional space; 1D can be used to denote the
real line.

If we take the metric space 2D or 3D, we can
easily represent a unit sphere graph G in the space
itself. We represent the vertices by the points and
draw a line segment from v_i to v_j for any pair of
adjacent vertices of the graph G.

Here are some specific examples:

Example 1 *Let us select the following points in
the Euclidean plane:* (x, y), $x \in \{1, 2, \ldots, a\}$, $y \in$

Figure 1: The grid graph $Gr(3,5)$. This is the same as the Cartesian product of paths P_3 and P_5.

Figure 2: The strong product of paths P_3 and P_5.

$\{1, 2, \ldots, b\}$. *Hence $n = ab$. Let $r = 0.5$. The unit sphere graph is the well-known $a \times b$ grid graph $Gr(a, b)$. The grid graph is also known in graph theory as the Cartesian product of the paths P_a and P_b. Figure 1 shows the case for $a = 3$ and $b = 5$.*

In order to understand better the nature of unit sphere graphs, one can do at least two experiments. One can keep the set of vertices V fixed and change the unit r. For $0 < r < 0.5$ we get the graph consisting of ab isolated vertices and no edges. For $0.5 \leq r < \sqrt{2}/2$ we get the grid graph (Figure 1). For $\sqrt{2}/2 \leq r < 2$ we get the graph that is obtained from $Gr(a, b)$ by adding the pair of diagonals in each unit square (Figure 2).

This graph is also known as the *strong product* of paths P_a and P_b. Obviously a unit sphere graph with a smaller value of r is a subgraph of the unit sphere graph with a larger unit sphere value. However, to determine the number of distinct unit sphere graphs even for regular configurations of points such as the grid configuration seems to be nontrivial. For a given pair of integers $0 \leq a \leq b$ one can write a computer program that will determine the number $t(a, b)$ of distinct unit sphere graphs. For a given set V one can do the same thing and determine the number of distinct unit sphere graphs $t(V)$. One way of getting the result is to calculate the $n \times n$ symmetric distance matrix $D(V)$ with 0 on the main diagonal in which the entry in the i-th row and j-th column is given as the distance between v_i and v_j. Then $t(V)$ is simply the number of distinct values in $D(V)$. Since there are at most $n(n-1)/2$ edges in a graph with n vertices, there are at most $1 + n(n-1)/2$ distinct unit sphere graphs. If we select n points in the real line 1D with coordinates: $1, 2, 4, 8, \ldots, 2^{n-1}$ we can see that all $n(n-1)/2$ differences are distinct. The points give rise to the maximum poss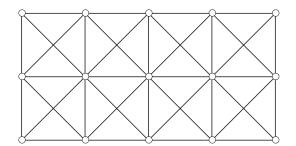ible number of unit sphere graphs. If we select n equidistant points on the line, we get only n distinct unit sphere graphs. The reader may prove that we cannot reduce this number. In 2D we can do much better if we select the points as the vertices of the regular n-gon. There are only $1 + \lfloor n/2 \rfloor$ unit sphere graphs. For a given n, find the minimum in 2D and also in 3D.

Unit sphere graphs admit various generalizations and modifications. The most obvious one would be that each point v_i carries its own radius r_i. The balls $B_i := B(v_i, r_i)$ now have different radii; however, the condition remains the same. One can consider the case of n radio stations with different ranges broadcasting on various frequencies. There is interference if a listener can listen to two different radio stations broadcasting on the same frequency. We may model the situation by a sphere graph. Each vertex of the graph is assigned a frequency (color). The broadcasting has no interference if and only if the corresponding graph is properly colored (no two adjacent vertices are assigned the same color). Minimizing the number of frequencies is equivalent to finding the chromatic number of the graph (i.e. the least number of colors used in a proper coloring of the graph).

When setting up the model one has to select the radii. There is a natural choice for the radius of a vertex; let r_i of the vertex v_i be the distance to the nearest neighbor of v_i. This is how we get the *nearest neighbor* graphs.

Here is another possible generalization: To each point v_i we associate two radii $r_i \leq R_i$ and two balls $b_i := B(v_i, r_i), B_i := B(v_i, R_i)$. Let b_i^0 denote the interior of the ball b_i. The adjacency condition now reads:

$$v_i \equiv v_j \text{ if and only if } b_i^0 \cap b_j^0 = \emptyset \text{ and } B_i \cap B_j \neq \emptyset$$

Here are two examples:

Example 2 *Chemistry.   We may model some molecules by assigning radii to various atoms. By*

placing atoms in a plane (or space) we then automatically get the graph of the molecule. Several computer programs for molecular dynamics such as RasMol [61] use such models; see also [55]. It can be shown that all benzenoid graphs can be described as unit sphere graphs in 2D. A graph is called a benzenoid graph[1] if it can be obtained by selecting a connected subset of hexagons in an infinite planar hexagonal lattice (representing graphite).

Example 3 *Touching coins and touching pennies, [31]. Given a set of coins $c_1, c_2, \ldots, c_n$ in the plane, we may define the graph that has the n vertices in the centers of $c_1, c_2, \ldots, c_n$ and the i-th and j-th vertices are adjacent if and only if the coins c_i and c_j touch. In 1935 it was shown by Koebe that any planar graph can be realized as a coin graph. If we impose an additional condition that all coins have equal radius we obtain the so-called penny graph.*

Unit sphere graphs are a special case of intersection graphs. Given a family of sets $\{S_1, S_2, \ldots, S_n\}$ we define a graph on n vertices as follows: the vertex set is $\{S_1, S_2, \ldots, S_n\}$. Two vertices S_i and S_j are adjacent iff $S_i \cap S_j \neq \emptyset$. By selecting various geometric objects we get interesting families of graphs. For instance, the so-called *interval graphs* are intersection graphs of finite families of line segments in the 1D line.

If we select a direction on each edge of graph G the so-called *directed graph* or *digraph* D is obtained. Each digraph D corresponds to a binary relation R on the set of vertices of D. Two vertices a and b are related by R if and only if there is a directed arc in D from a to b. Graph G has a *transitive orientation* if the binary relation corresponding to the digraph is transitive.

Interval graphs are characterized by the following structural theorem, where a cycle in a graph is called *chordless* if it is an induced subgraph: no diagonal is an edge of the graph.

Theorem 1 *G is an interval graph if and only if it has no chordless cycle C_n, for $n > 3$ and its complement admits a transitive orientation.*

Unit sphere graphs in 1D are called unit interval graphs. They were characterized by F. S. Roberts, [60].

[1] In chemistry a benzenoid graph is sometimes defined in a slightly different way. Namely, it is required to have at least one Kekule structure, i.e. a perfect matching. Also, a long string of hexagons that winds in a spiral may be considered a benzenoid even though distinct hexagons may project to the same hexagon in the graphite lattice.
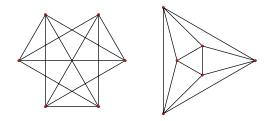
Theorem 2 *G is a unit interval graph if and only if it is an interval graph and has no induced $K_{1,3}$ subgraph, where $K_{n,m}$ is the complete bipartite graph with n vertices in one part and m vertices in the other part.*

It would be interesting and useful to characterize the unit sphere graphs in 2D and 3D. For instance, all platonic graphs arise as unit sphere graphs in 3D. One has to take the vertices of the corresponding platonic solid and radius r the half of the edge length. It appears that one cannot get the cube graph Q_3 as a unit sphere graph in 2D.

Finally, we defined a unit sphere graph for any metric space. Any connected graph admits the structure of a metric space. The points are vertices and the distance is the length of the shortest path from one vertex to another. It would be interesting to see what unit sphere graphs arise from a given connected graph. Let G be a graph and let G^i denote the graph obtained from G by joining two vertices u and v by an edge if and only if the distance between u and v in G is at most i. It can be shown that the unit sphere graphs arising from G are precisely all induced subgraphs of $G^i, i = 1, 2, \ldots$. Even among specialists in graph theory it is not widely known that a graph can allow additional metrics. Besides the common shortest path metric we also have the *resistance distance metric* and other metric alternatives; see [40] and [41].

3 Polyhedra and Graphs

In the previous section we found a way from a polyhedron to a graph via unit sphere graphs. There is a much easier way of getting a graph from a polyhedron, obtained by taking the one-skeleton, i.e. the graph composed of vertices and edges of the polyhedron. We keep the vertices and the edges and forget all the other information (e.g. the facial structure or metric structure.) This route is quite interesting and gives among other things a very important family of graphs. A graph G is 3-connected if deletion of any pair of vertices results in a connected subgraph. It is planar if it can be drawn in the plane without crossings. Let us call a graph *polyhedral* if it is a one-skeleton of a convex polyhedron.

Theorem 3 *(Steinitz [63].) The one-skeleton of an arbitrary convex polyhedron is a planar 3-connected graph and each planar 3-connected graph is polyhedral.*

Figure 3: Two alternative drawings of $K_{2,2,2}$ (the graph of the octahedron).

Example 4 *The one-skeleton of the octahedron is the complete tripartite graph $K_{2,2,2}$ on 6 vertices. One way of drawing this graph is to take the so-called Schlegel diagram of the octahedron. A Schlegel diagram of a convex polyhedron is obtained by first selecting a face and then using a stereographic projection from the center of that face onto a plane. Thus the selected face becomes the infinite face of the plane graph, which is the Schlegel diagram. For aesthetic reasons the resulting drawing is then homeomorphically changed in such a way that the faces are not accumulated too much in the center. However, we should always bear in mind that the graph G does not carry explicit information about the position of its vertices. We can represent the same graph by different drawings; see Figure 3.*

The route back from a graph to a polyhedron is not so obvious. Recovering hidden or missing information is never as easy and obvious as throwing away information.

If we allow non-convex polyhedra we may get different polyhedra giving the same one-skeleton. The *uniform polyhedron* of Figure 4 is a model of a projective plane. In [66] it is called a *heptahedron*. However, it is better known as a *tetrahemihexahedron*; see [49], where you can find more information about and illustrations of uniform polyhedra. It has 6 vertices, 12 edges, 4 triangles and 3 squares. Its one-skeleton is again $K_{2,2,2}$; see Figure 3.

Figure 5 shows its embedding in the projective plane. The antipodal points of the disk are identified.

If we start with a cuboctahedron, we can obtain two different polyhedra depending on what type of faces are replaced by hexagons.

By keeping all triangles and replacing the quadrilaterals by main hexagons, we get an *octahemioctahedron* whose map on torus is shown in Figure 6. On the other hand one may keep quadrilaterals and
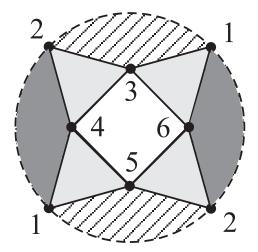

Figure 5: $K_{2,2,2}$ embedded in the projective plane with 4 triangles and 3 squares. The antipodal points on the dotted border are identified.

remove triangles. The polyhedron is called a *cubohemioctahedron* [49]. It consists of 6 quadrilaterals and 4 hexagons.

By keeping information about faces, we get the so-called *2-skeleton* of a polyhedron. It has vertices, edges, and faces and all the information about how to glue the pieces together.

Informally, a *map* is a collection of fused polygons. More rigorously, a *map* is a collection of polygons with directed sides such that the total number of sides is even together with an involution on the set of sides without fixed points which determines how the sides are pairwise glued (respecting the orientation.) If the resulting complex is connected, we get a surface. (For exact definition and more examples, see the book by Ringel [59]; see also [67].)

4 Operations on Maps

A map is a combinatorial representation of a closed surface. There are several equivalent combinatorial descriptions available for maps. In the computer package Vega [57], we implemented a series of operations on maps. This enables us to produce new maps from old ones. In turn, we can get new polyhedra or new graphs.

Here we present some operations on maps; all of them are explained via examples in the figures. We consider only connected maps.

- Du: *Dual.* This operation is well-known for planar graphs. However, it can be generalized

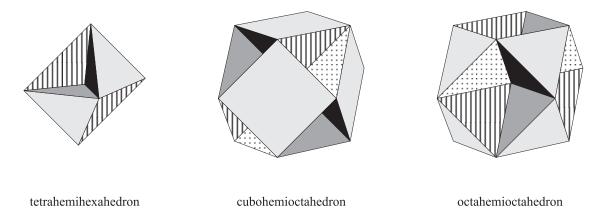tetrahemihexahedron   cubohemioctahedron   octahemioctahedron

Figure 4: The heptahedron or tetrahemihexahedron is not convex. It is self-intersecting and even non-orientable as a map in the projective plane. Its one-skeleton is the graph on Figure 3. Octahemioctahedron and cubohemioctahedron share with cuboctahedron the same one-skeleton shown on Figure 10.
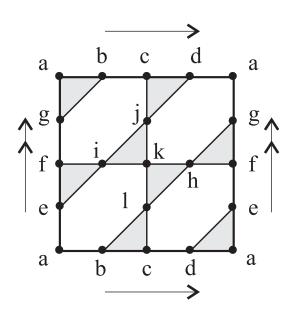

Figure 6: The map of octahemioctahedron in torus with 8 triangles and 4 hexagons. The arrows and double arrows show how to identify the sides of a rectangle in order to form the torus.

for maps in other surfaces. It is also known as the *Poincaré dual*. The dual map $Du(M)$ is built from the original map M as follows: we put a vertex of $Du(M)$ in the center of each face of M. For each edge e of M we produce its dual $Du(e)$ so that $Du(e)$ connects the vertices corresponding to the faces of M that have e on the common boundary. We place the vertex $Du(M)$ in the same surface as M in such a way that the faces of $Du(M)$ correspond to the vertices of M. This means that the dual edges are traversed along faces in the same cyclic order as the original edges are traversed cyclically around a vertex. It can be shown that $Du(Du(M)) = M$.

Let us consider three examples that will serve us also for other operations.

1. The cube Q_3 in the sphere: $v = 8$, $e = 12$, $f = 6$. The dual is the octahedral graph $K_{2,2,2}$ in the sphere: $v = 6$, $e = 12$, $f = 8$; see Figure 8.

   A projection of a sphere-like polyhedron on a plane is sometimes called a *Schlegel diagram*. Such a projection is similar to the so-called stereographic projection in which exaclty one point on a sphere, called the *center*, is mapped to infinity. In a polyhedron the center is usually taken either at a vertex, at the center of an edge or at a center of a face, see Figure 7.

2. The *bouquet* B_n of n circles is a graph with n loops attached to a single vertex. The bouquet of one circle B_1 in the projective
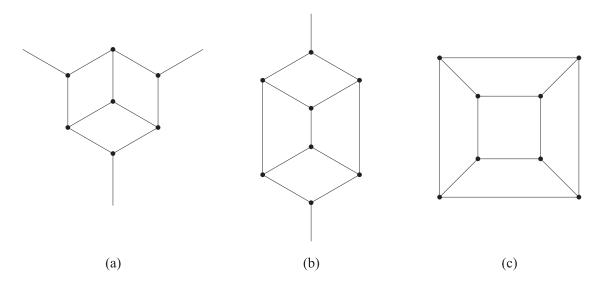
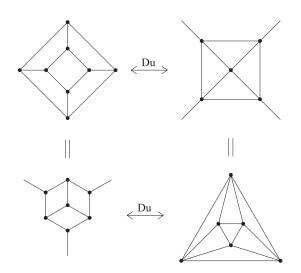Figure 7: Schlegel diagrams of cube (a) centered at a vertex, (b) centered at an edge, (c) centered at a face.

Figure 8: The cube and its dual, the octahedron.

plane: $v = 1$, $e = 1$, $f = 1$. It is self-dual: $v = 1$, $e = 1$, $f = 1$.

3. Another example of a self-dual map is the tetrahedron K_4 in the sphere.

4. K_4 in the torus: $v = 4$, $e = 6$, $f = 2$. One face is a quadrilateral and the other one is a hexagon. The dual graph has two vertices; one vertex has a double loop and there are four parallel edges between the two vertices: $v = 2$, $e = 6$, $f = 4$. All faces are triangles.

If v, e, f are the parameters of the original and v', e', f' are the parameters of the transformed map we have the relations:

$$v' = f$$
$$e' = e$$
$$f' = v.$$

- Su1: *1-dimensional subdivision.* This is the simplest of all. We subdivide each edge by inserting a vertex at the midpoint of each edge thus splitting the edge in two; see Figure 9.

  1. The cube Q_3 in the sphere: $v = 8$, $e = 12$, $f = 6$. The 1-dimensional subdivision has the parameters: $v = 20$, $e = 24$, $f = 6$.

  2. The bouquet of one circle B_1 in the projective plane: $v = 1$, $e = 1$, $f = 1$. Its subdivision Su1 is the cycle C_2 in the same surface: $v = 2$, $e = 2$, $f = 1$.
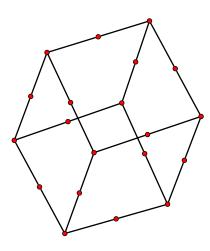
Figure 9: The subdivided cube.

Figure 10: The cuboctahedron, the medial of the cube.

3. K_4 in the torus: $v = 4$, $e = 6$, $f = 2$. The subdivision graph has parameters $v = 10$, $e = 12$, $f = 2$. All faces have twice as many edges as before.

If v, e, f are the parameters of the original and v', e', f' are the parameters of the transformed map we have the relations:

$$v' = v + e$$
$$e' = 2e$$
$$f' = f.$$

- Pa : *Parallelization.* Here we replace each edge by a pair of parallel edges forming a digon on the surface. Instead of giving this description we could define Parallelization formally as: $Pa(M) := Du(Su1(Du(M)))$

$$v' = v$$
$$e' = 2e$$
$$f' = e + f$$

- Si : *Simplification.* This operation is in a sense the inverse to the operation of Su1. It removes all vertices of valence 2 but leaves the graph (and the map) topologically the same. The only exception is the bouquet B_1 which does not allow further reductions.

- PSi : *Parallel Simplification.* This operation is in a sense the inverse to the operation of Pa. It removes all digons by changing them into a single edge. $PSi(M) := Du(Si(Du(M)))$
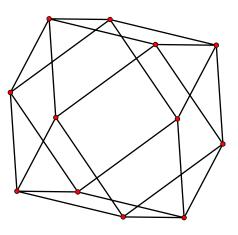
- Me : *Medial.* This is probably the most important transformation of a map and is not so simple. The new vertices are the midpoints of the original edges. New vertices are adjacent if and only if the two original edges span an angle; i.e. the two edges must be incident and consecutive when traversing the rotation about their common vertex in the map. The medial graph is thus a subgraph of the *line-graph*. For the definition of line-graph, see for instance, [68]. In the line-graph each original vertex gives rise to a complete graph; in the medial graph it only gives rise to a cycle.

If v, e, f are the parameters of the original and v', e', f' are the parameters of the transformed map we have the relations:

$$v' = e$$
$$e' = 2e$$
$$f' = v + f$$

1. The cube Q_3 in the sphere: $v = 8$, $e = 12$, $f = 6$. Its medial is the cuboctahedron and has the parameters: $v = 12$, $e = 24$, $f = 14$; see Figure 10.

2. The bouquet of one circle B_1 in the projective plane: $v = 1$, $e = 1$, $f = 1$. Its medial is B_2 in the same surface: $v = 1$, $e = 2$, $f = 2$.

3. K_4 in the torus: $v = 4$, $e = 6$, $f = 2$. The medial graph Me is obtained from $K_{2,2,2}$

by doubling 8 edges with one endpoint in the same color class with parameters: $v = 6$, $e = 12$, $f = 6$. There are 4 triangles, one quadrilateral and one octagon.

Medials have interesting properties:

- Each one is isomorphic to the medial of the dual:

$$Me(G) = Me(Du(G))$$

- All are 4-valent and their duals are bipartite.

- The structure of the map and its dual are visible in the medial.

- Face lengths and vertex valencies are readily visible in the medial.

- The map and its dual occur symmetrically in the medial.

- Tr: *Truncation*

  Truncation can be first described intuitively. We cut off the neighborhood of each vertex by a plane "close" to the vertex that meets each edge incident to the vertex. Using transformations from above we may define truncation Tr to be $Tr(G) = PSi(Me(Su1(G)))$. It is the medial of a 1-subdivided map. That would introduce parallel edges and digons. That is why we insist that the operation is followed by parallel simplification. Compare [20].

- Su2: *2-dimensional subdivision*

  The 2-dimensional subdivision of a graph is obtained by adding a vertex in the center of each face and joining it by edges to the vertices of the original face; see Figure 11.

  There is also an interesting connection between truncation and the 2-dimensional subdivision, namely, $Tr(Du(G)) = Du(Su2(G))$; see for instance [40]. Therefore, $Su2$ can be defined in terms of truncation:

$$Su2(G) = Du(Tr(Du(G)))$$
$$= Du(PSi(Me(Su1(Du(G))))).$$

- BS: *Barycentric subdivision*

  The barycentric subdivision is a composite operation: It is a 2-dimensional subdivision of the 1-dimensional subdivison.

$$BS(G) = Su2(Su1(G))$$
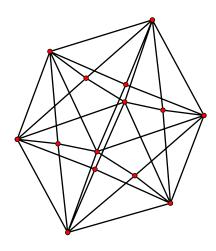$$= Du(PSi(Me(Su1(Du(Su1(G)))))).$$

Figure 11: The two-dimensional subdivision of the cube.

The barycentric subdivision has an important role in topology and its dual is also very interesting, as it is a cubic graph and thus much easier to visualize.

- Pe: *Petrie Dual*

  The Petrie dual is the first operation that keeps the 1-skeleton fixed and only changes the faces of the map. New faces are composed of all left-right walks on the surface: every two consecutive edges of the new faces are also consecutive edges of the old faces. However, no three consecutive edges of new faces form consecutive edges of the old faces. It can be shown that it is indeed a "dual" in the sense that $Pe(Pe(G)) = G$. The Petrie dual is a powerful operation as it can turn an orientable surface into a nonorientable one and vice versa.

  For instance, the Petrie dual of the ordinary cube Q_3 gives its embedding in the torus with all hexagonal faces. However, there is another, different hexagonal embedding of Q_3 in torus; see Figure 12. This may run counter our intuition, since Q_3 in particular has only one drawing in the sphere.

- R2: *Rotation Square*

  The rotation square changes faces. It is well-defined only for graphs that have all vertices of odd valence. The map is completely defined if we specify its *rotation scheme*, i.e. at
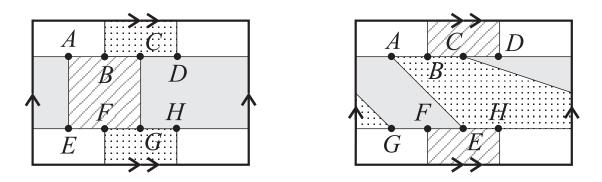
Figure 12: Two all-hexagonal drawings of the cube Q_3 on the torus.

each vertex we give the cyclic order of incident edges. Rotation square takes the square of the overall permutation. If $(e_1, e_2, \ldots, e_s)$ is the local rotation at a vertex, then we have in the rotation square the following sequence $(e_1, e_3, e_5, \ldots, e_2, e_4, \ldots)$. That is why we need s to be odd.

- S2: *Embedded Square*

  The idea behind the embedded square is similar to the idea of the rotation square; however, the construction is quite different and the resulting graph is quite different from the original. The graph is obtained by keeping the vertices of the original and adding an edge at each angle. If we have a face in the original that has $(v_1, v_2, \ldots, v_s)$ as a sequence of vertices then the new edges are $v_1 - v_3, v_2 - v_4, v_3 - v_5, \ldots$

- Sn1 and Sn2: *Snub*

  There are two snub operations. First we take two consecutive medials $Me(Me(G))$. The resulting map is 4-valent and also equipped with a collection of quadrilaterals, arising from vertices of the first medial operation $Me(G)$, such that each vertex of $Me(Me(G))$ belongs to two quadrilaterals. By inscribing a diagonal in one of the quadrilaterals one induces diagonals in all remaining quadrilaterals. If the other initial diagonal is selected the resulting map is $Sn2(G)$ instead of $Sn1(G)$. When Sn1 and Sn2 are isomorphic we simply have a snub Sn. For instance, for a tetrahedron T, $Sn(T) = Sn1(T) = Sn2(T)$ is topologically equivalent to the icosahedron I but $Sn1(I) \neq Sn2(I)$. There are five Platonic polyhedra, with all vertices, all edges, and all faces mutually equivalent. There are 13 Archimedean polyhedra in which all vertices are equivalent but neither
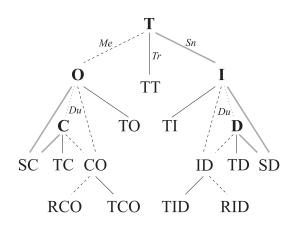

Figure 14: Evolution of the Platonic and Archimedean polyhedra from the tetrahedron.

the edges nor the faces are. All Platonic and Archimedean polyhedra can be obtained from the tetrahedron T by some sequence of operations that we have introduced; see Figures 13 and 14.

- Le: *Leapfrog*

  Leapfrog [20] is a term coined by chemists. It represents a composite operation. It is the truncation of the dual:

  $$Le(G) = Tr(Du(G))$$
  $$= PSi(Me(Su1(Du(G)))).$$

  It can be described in an intuitive way. Recall how we envision truncation. The process of truncation involves a collection of planes, one for each vertex, that cut off parts of the polyhedron close to each vertex. If we "move" these planes towards the center of polyhedron, each original edge is diminished and is at a certain

Symbol	Polyhedron	Operation	Formula
T	Tetrahedron	Primitive	—
O	Octahedron	Medial	Me(T)
C	Cube(Hexahedron)	Dual	Du(O) = Du(Me(T))
I	Icosahedron	Snub	Sn(T)
D	Dodecahedron	Dual	Du(Sn(T))
TT	Truncated tetrahedron	Truncation	Tr(T)
TO	Truncated octahedron	Truncation	Tr(O) = Tr(Me(T))
TC	Truncated cube	Truncation	Tr(C) = Tr(Du(Me(T)))
TI	Truncated icosahedron	Truncation	Tr(I) = Tr(Sn(T))
TD	Truncated dodecahedron	Truncation	Tr(D) = Tr(Du(Sn(T)))
CO	Cuboctahedron	Medial	Me(C) = Me(Me(T))
ID	Icosidodecahedron	Medial	Me(I) = Me(Sn(T))
TCO	Truncated cuboctahedron	Truncation	Tr(CO) = Tr(Me(Me(T)))
TID	Truncated icosidodecahedron	Truncation	Tr(ID) = Tr(Me(Sn(T)))
RCO	Rhombicuboctahedron	Medial	Me(CO) = Me(Me(Me(T)))
RID	Rhombicosidodecahedron	Medial	Me(ID) = Me(Me(Sn(T)))
SC	Snub cube	Snub	Sn(C) = Sn(Du(Me(T)))
SD	Snub dodecahedron	Snub	Sn(D) = Sn(Du(Sn(T)))

Figure 13: Derivation of the Platonic and Archimedean polyhedra from the tetrahedron.

moment reduced to a single point, the midpoint. The polyhedron obtained at that moment is the medial. If we continue the process beyond that point, we obtain the leapfrog. Similar intuitive processes can be applied to an arbitrary map yielding the same result.

Patchwork

Consider the polyhedron with the seams of the traditional soccer ball as edges. This is the truncated icosahedron, one of the trivalent Archimedean polyhedra, having 60 vertices and faces that are pentagons and hexagons. Furthermore, the pentagons are colored black and the hexagons white as in the soccer ball. The black faces are vertex disjoint but each of the 60 vertices lies on the boundary of a black face. Such a collection of faces is called a *patchwork*. There are many trivalent polyhedra with pentagonal and hexagonal faces. They are called *fullerenes*. The name was suggested by Harry Kroto, one of the 1996 Nobel prize winners and discoverers of C_{60}, which is a novel allotropic form of carbon different from the well-known forms graphite and diamond. They are named after the architect Buckminster Fuller, in appreciation for his pioneering work on design and construction of huge domes based on geometrical considerations. A fullerene with a patchwork is called a *generalized soccer ball*. Note that in generalized soccer balls in addition to black pentagons there will be some black hexagons. The following is a characterization

[20] of generalized soccer balls:

Theorem 4 *A fullerene is a generalized soccer ball if and only if it is a leapfrog of another fullerene.*

It is known that fullerenes with abutted pentagons are not chemically stable and are therefore of little interest while generalized soccer balls have no abutted pentagons.

Triangulations

If a polyhedron has some non-triangular faces, we may introduce additional diagonals until all faces are triangles. The corresponding graph is known as a *maximally planar graph* or *triangulation*. Note that introduction of any additional edge to such a graph necessarily produces a non-planar graph, i.e., a graph that cannot be drawn in the plane without crossing of lines.

Diagonal flips [52]

It can be shown that any two triangulations on the same number of vertices are equivalent under diagonal flips: this means that one can start with one triangulation and obtain any other by a series of diagonal flips.

The dual of a triangulation is a cubic polyhedron. The dual operation of the diagonal flip is sometimes referred to in chemistry as the Stone-Wales transformation.
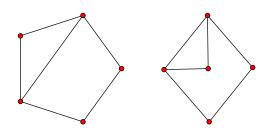
Figure 15: Two embeddings of a graph in the plane.

Before we leave the subject let us think a bit about the analogy of a self-intersecting projective planar polyhedron and a drawing of a non-planar graph in the plane. In both cases topologists would call such a phenomenon an *immersion*. If there are no singularities (no self-intersections) then we speak about *embeddings*. Clearly only planar graphs allow embeddings in the plane. Actually each planar graph without loops and parallel edges admits a straight-line embedding in plane—this is known as Fary's Theorem—although the embedding is not necessarily unique as shown in Figure 15.[2]

On the other hand, each graph can be embedded in 3D using only straight-line segments as edges. We can pose the following optimization problem. Let us take the three-dimensional grid of the shape of the cube with $n \times n \times n$ points. The problem is to select k out of the n^3 points in such a way that the vertices of the complete graph K_k can be placed on the selected points and that would result in the embedding of K_k in 3D with line-segments representing edges meeting only at points representing vertices. For a given n what is the largest possible k? For $n = 1$ it is obviously $k = 1$, for $n = 2$ we get $k = 5$. It seems that for $n = 3$ we get $k = 6$. What is the value of k for $n = 4$?

5   Symmetry and Orbits

Platonic and Archimedean polyhedra are highly symmetric. Each of them has indistinguishable vertices. However, the edges of Archimedean polyhedra are not all alike. This phenomenon can be understood by the concept of *orbits*. We will explain this concept first in graphs.

Let $G = (V, E)$ be a graph with the vertex set V and edge set E. A permutation $\pi : V \to V$ is

---

[2] By Whitney's theorem, any planar 3-connected graph admits a unique embedding on the sphere. A graph G other than the triangle K_3 is 3-connected if the graph obtained by deleting any two vertices from G remains connected.

an *automorphism* of G if it preserves adjacencies: $(u, v) \in E$ if and only if $(\pi(u), \pi(v)) \in E$. The automorphisms of G form a group that we denote by $Aut(G)$. Two vertices u and v of G are *indistinguishable* if one can be mapped to the other by some graph automorphism. The set of indistinguishable vertices form an *orbit* of $Aut(G)$. If all vertices of G are indistinguishable we say that G is *vertex-transitive*. We may also view automorphisms of G acting on the edges of G.

The graph of a regular prism is obviously vertex-transitive but in general not edge-transitive. It is impossible to distinguish among the vertices, but one can tell apart lateral edges from the base edges unless the prism is a cube.

There are graphs that have all edges indistinguishable but do not have all the vertices alike. One of the graphs is the so-called Folkman graph. The Folkman graph is therefore edge-transitive but not vertex-transitive. See Figure 16.

There is another notion that we will use later; it is called arc-transitivity. A graph G is called *arc-transitive* if for any pair of edges $(u, v) \in E$, $(u', v') \in E$ one can find two automorphisms π and π' such that $\pi(u) = u', \pi(v) = v'$ and $\pi'(u) = v'$ and $\pi'(v) = u'$. Hence the notion of arc-transitivity is stronger than edge-transitivity. It means that we can map any edge to any other edge in an arbitrary direction. Clearly arc-transitivity implies edge-transitivity.
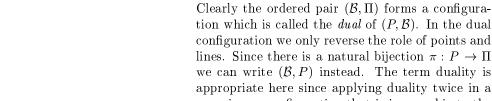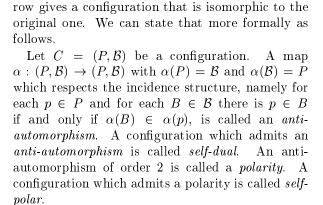
6   Configurations and Levi Graphs

A *configuration* of type (n_r, b_k) is an ordered pair $(P, \mathcal{B})$, consisting of a set of n *points* $P = \{p_1, \ldots, p_n\}$ and a collection of b *lines (blocks)* $\mathcal{B} = \{B_1, \ldots, B_b\}$ with $B_i \subseteq P$, for each $i = 1, \ldots, n$, and $\pi(p_j) := \{B \in \mathcal{B} | p_j \in B\}$, for each $j = 1, \ldots, n$, such that

1. Each line contains k points: $|B_i| = k$, for each $i = 1, \ldots, b$,

2. Each point lies on r lines: $|\pi(p_j)| = r$, for each $j = 1, \ldots, n$,

3. Two different points are connected by at most one line: $|B_i \cap B_j| \leq 1$, for each $i \neq j, i = 1 \ldots, b, j = 1, \ldots, b$.

The ordered pair (p, B) with $p \in P, B \in \mathcal{B}$ and $p \in B$ is called a *flag*. If $k = r$ and hence $n = b$ (see, for instance [18]) the configuration is called *symmetric* and its type is denoted by n_k.

Let $\Pi := \{\pi(p)|p \in P\}$, where π is defined above. Clearly the ordered pair $(\mathcal{B}, \Pi)$ forms a configuration which is called the *dual* of $(P, \mathcal{B})$. In the dual configuration we only reverse the role of points and lines. Since there is a natural bijection $\pi : P \to \Pi$ we can write $(\mathcal{B}, P)$ instead. The term duality is appropriate here since applying duality twice in a row gives a configuration that is isomorphic to the original one. We can state that more formally as follows.

Let $C = (P, \mathcal{B})$ be a configuration. A map $\alpha : (P, \mathcal{B}) \to (P, \mathcal{B})$ with $\alpha(P) = \mathcal{B}$ and $\alpha(\mathcal{B}) = P$ which respects the incidence structure, namely for each $p \in P$ and for each $B \in \mathcal{B}$ there is $p \in B$ if and only if $\alpha(B) \in \alpha(p)$, is called an *anti-automorphism*. A configuration which admits an *anti-automorphism* is called *self-dual*. An anti-automorphism of order 2 is called a *polarity*. A configuration which admits a polarity is called *self-polar*.

Let C be a configuration; then $A(C)$ denotes the group of all its automorphisms and anti-automorphisms, while $Aut(C)$ denotes the group of its automorphisms. Then $Aut(C)$ is a subgroup of $A(C)$. If C is self-dual, it is a proper subgroup; otherwise, $Aut(C) = A(C)$.

If $Aut(C)$ is transitive on points P, lines $\mathcal{B}$, or flags, C is called *point-*, *line-*, or *flag-transitive* respectively.

A *triangle* of a configuration consists of three points, say a, b, and c, such that each of the three pairs $\{a,b\}$, $\{b,c\}$, and $\{a,c\}$ is contained in a line. A configuration that has no triangles is called a *triangle-free configuration*.
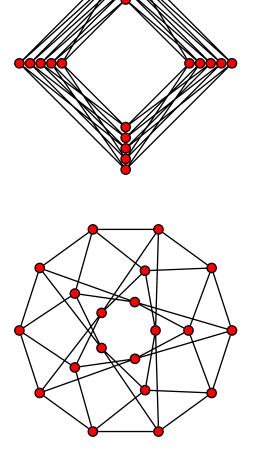
If there is a cyclic subgroup of $Aut(C)$ which acts transitively on P, the configuration C is called *cyclic*. Cyclic configurations can be described in a concise way. We only have to specify the number of points n and provide the 0-th line. The i-th line is then obtained by adding i (mod n) to the index of each element of the 0-th line.

The *Levi graph* $L = L(P, \mathcal{B})$ of a configuration was introduced by Coxeter in 1950, see [12]. It is a bipartite graph with "black" vertices P and "white" vertices $\mathcal{B}$ and with an edge between $p \in P$ and $B \in \mathcal{B}$ if and only if $p \in B$. Note that dual configurations have the same Levi graph but the roles of black and white vertices are interchanged.

Complete information about the configuration can be recovered from its Levi graph with a given black and white coloring of vertices. Hence counting configurations can be done via careful counting of Levi graphs. Two configurations $(P, \mathcal{B})$ and $(P', \mathcal{B}')$ are isomorphic if and only if there is an iso-

Figure 16: The standard drawing of the Folkman graph and another drawing of the same graph.

morphism between their Levi graphs $L(P, \mathcal{B})$ and $L(P', \mathcal{B}')$ that maps black vertices into black vertices.

It is well-known (see [12]) that a graph G is a Levi graph of some n_3 configuration if and only if:

1. G is cubic

2. G is bipartite

3. The length of the shortest cycle in G, the girth, is at least 6.

Table 17 shows the correspondence between properties of configurations and their Levi graphs.

Recently the number of n_3 configurations up to $n \leq 18$ was computed in [4].

Example 5 *Each regular graph of valence k without loops and multiple edges can be viewed as an (n_k, b_2) configuration of points and lines. Vertices correspond to points and edges correspond to lines (line segments). The corresponding Levi graph is the subdivision graph of the original graph.*

Example 6 *Take the equilateral triangle with all three altitudes and the inscribed circle. The configuration consists of the 7 points, 6 line segments and the circle; see Figure 18. The configuration graph is the well-known Heawood graph; see Figure 19. This graph on 14 vertices has shortest cycle of length 6. The configuration is interesting as it represents the smallest model of a finite projective plane, the well-known Fano plane. This is the unique and smallest configuration of points and lines.*

Any abstract configuration can be described as a collection of sets. The elements represent points and the sets represent lines. The Fano configuration can thus be described as:

$$\{\{1, 2, 6\}, \{2, 3, 4\}, \{1, 3, 5\}, \{1, 4, 7\},$$
$$\{2, 5, 7\}, \{3, 6, 7\}, \{4, 5, 6\}\}$$

Clearly it is isomorphic to the configuration:

$$\{\{1, 2, 3\}, \{1, 4, 5\}, \{1, 6, 7\}, \{2, 4, 6\},$$
$$\{2, 5, 7\}, \{3, 4, 7\}, \{3, 5, 6\}\}$$

Since the Fano configuration is cyclic, it can also be generated by $n = 7$ and 0-th row $\{0, 2, 6\}$.

$$\{\{0, 2, 6\}, \{1, 3, 0\}, \{2, 4, 1\}, \{3, 5, 2\},$$
$$\{4, 6, 3\}, \{5, 0, 4\}, \{6, 1, 5\}\}$$

It can be verified that the Fano configuration is self-dual; actually it is self-polar.
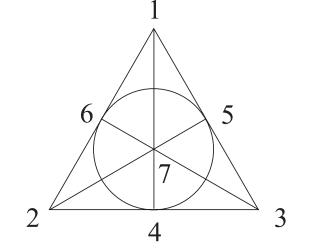

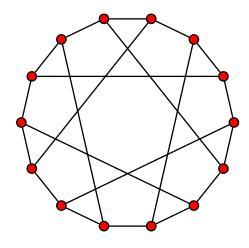Figure 18: The Fano configuration with 7 points and 7 lines. The seventh line is drawn as a circle.

Figure 19: The Levi graph of the Fano configuration, also known as the Heawood graph or the 6-cage.

Configuration $(P, \mathcal{B})$	Levi graph $L(P, \mathcal{B})$
incidence structure	bipartite graph
1-configuration [27]	girth ≥ 6
n_r, b_k	semi-regular, girth ≥ 6
n_3	bipartite, cubic, girth ≥ 6
points	black vertices
lines (blocks)	white vertices
no triangles	girth ≥ 8
self-dual	$\gamma \in Aut(L)$ swaps black and white vertices
self-polar	$\gamma \in Aut(L)$ of order 2 swaps black and white vertices
indecomposable	connected
incidence matrix	bi-adjacency matrix
point-transitive	all black vertices in the same orbit under $Aut(L)$
line-transitive	all white vertices in the same orbit under $Aut(L)$
flag-transitive	edge-transitive
flag-transitive, self-dual	arc-transitive
point-transitive, self-dual	vertex-transitive
cyclic	Haar graph of girth ≥ 6

Figure 17: Properties of configurations and their Levi graphs.

Example 7 *Take three lines a, b, and c forming a triangle ABC. The corresponding configuration graph is the complete bipartite graph $K_{3,3}$. In general, each n-gon defines a self-dual configuration of type n_2.*

Here is another example:

The Möbius-Kantor configuration is the only 8_3 configuration. It is also transitive and self-dual. It can be shown that the Möbius-Kantor configuration cannot be realized in the real projective plane. It can be realized in the complex projective plane. Figure 20 shows four drawings of its Levi graph. The top left drawing reminds us of the well-known Petersen graph; see Figure 27. That is why we introduce the family of generalized Petersen graphs.

7 Generalized Petersen Graphs and Haar Graphs

For a positive integer $n \geq 3$ and $1 \leq r < n/2$, *the generalized Petersen graph $GP(n, r)$* has vertex set $\{u_0, u_1, \ldots, u_{n-1}, v_0, v_1, \ldots, v_{n-1}\}$ and edges of the form $u_i v_i, u_i u_{i+1}, v_i v_{i+r}, i \in \{0, 1, \ldots, n-1\}$ with arithmetic modulo n.

In [21] the automorphism group of $GP(n, r)$ was determined for each n and r. With the exception of the dodecahedron $GP(10, 2)$, the generalized Petersen graph $GP(n, r)$ is vertex transitive, if and only if $r^2 \equiv \pm 1 \pmod{n}$; see also [43]. It was also shown in [21] that $GP(n, r)$ is arc-transitive if and only if

$$(n, r) \in \{(4, 1), (5, 2), (8, 3), (10, 2),$$
$$(10, 3), (12, 5), (24, 5)\}.$$

Note that $GP(4, 1)$ is the cube Q_3. On the other hand, $GP(5, 2)$ is the Petersen graph and $GP(8, 3)$ is known as the Möbius-Kantor graph [8], since it is the Levi graph of the unique 8_3 configuration. Similarly, $GP(10, 3)$ is the Levi graph of the Desargues configuration 10_3 and $GP(12, 5)$ is the Levi graph of one of the 229 configurations of type 12_3; [27].

Recall that any cyclic configuration of type n_k can be described by n and the first line $T \subseteq \{0, 1, \ldots, n-1\}, |T| = k, 0 \in T$. This, in turn, can be put in one-to-one correspondence with a positive integer N via its binary notation:

$$N = b_0 2^{n-1} + \cdots + b_{n-2} 2 + b_{n-1}$$

by letting $t \in T$ if and only if $b_t = 1$. Hence the complete information about a cyclic configuration and its Levi graph can be encoded by a positive integer N. In this way we get a graph $H(N)$ for each integer N which is called the *Haar graph* of N; see [34], [33]. If its girth is at least 6 then $H(N)$ is a Levi graph of a cyclic configuration.

In order to make the definition clear, let us construct the Heawood graph as the Haar graph $H(69)$. Since 69 is written in binary as 1000101 we conclude that $H(69)$ contains 7 "black" vertices, say, $v_0, v_1, \ldots, v_6$ and seven "white" vertices $u_0, u_1, \ldots, u_6$. Furthermore, vertex v_0 is adjacent
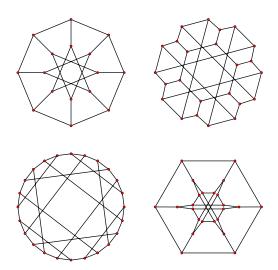
Figure 20: Four views of the Möbius-Kantor graph $GP(8,3) = H(133)$. A modification of the second drawing can be found in [36].

Figure 23: The Levi graph of the Cremona-Richmond configuration.

to vertices u_0, u_4, u_6 and vertex v_i is adjacent to the vertices $u_{0+i}, u_{4+i}, u_{6+i}$, where addition is taken mod 7. Note that we constructed in passing the Fano configuration:

$$\{\{0,4,6\}, \{1,5,0\}, \{2,6,1\}, \{3,0,2\},$$
$$\{4,1,3\}, \{5,2,4\}, \{6,3,0\}\}$$

Of course $GP(2m + 1, 1)$ does not have a Haar graph representation, whereas $GP(2m, 1) = H(2^{2m-1} + 3)$ and $GP(8,3)$, the only other generalized Petersen graph that is a Haar graph, is isomorphic to $H(133)$. Its automorphism group is of interest in topological graph theory; see [65].

We specialize the result from [45] to Levi graphs and combine it with common knowledge.

Proposition 1 ([45]) *$GP(8,3)$ is the only generalized Petersen graph that is a Levi graph of a cyclic configuration. The other two generalized Petersen graphs that are Levi graphs of point-transitive, self-dual configurations are $GP(10,3)$ and $GP(12,5)$.*

There are three 9_3 configurations of points and lines of type 9_3; see Figure 21. The most famous, called the Pappus configuration, is transitive and self-dual.

There are 10 configurations of points and lines of type 10_3. Only one of the 10 configurations is non-realizable in 3D (It is realizable over the quater-
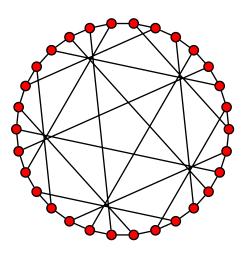
nions!). It is given as follows:

$$\{\{1,2,3\}, \{1,6,10\}, \{1,7,9\}, \{2,4,10\},$$
$$\{2,5,6\}, \{3,4,9\}, \{3,5,7\},$$
$$\{4,5,8\}, \{5,7,8\}, \{8,9,10\}\}.$$

The most important of the ten configurations is the Desargues configuration which is also transitive and self-dual; see Figure 22.

There are 31 configurations of type 11_3 and 229 of type 12_3. These facts were established more than hundred years ago by Daublebsky von Sterneck, [16], [17], although he missed one 12_3 configuration. Only recently it has been shown [64] that all these configurations admit realizations in 3D using integer coordinates.

The Cremona-Richmond configuration with 15 points and lines is the smallest n_3 configuration with no triangles [66]; see Figure 23.

For a more thorough introduction to the interesting area of configurations the reader is referred to the work of Harald Gropp; see, for instance, [24], [23], [26], [25]. Algorithmic aspects are covered in [6] and [64].

Configurations used to play important role in geometry. For instance, the following Theorem is one of the main results of a PhD thesis of renowned German geometer E. Steinitz [62]:

Theorem 5 *Each n_3 configuration can be drawn in a plane with at most one curved line.*
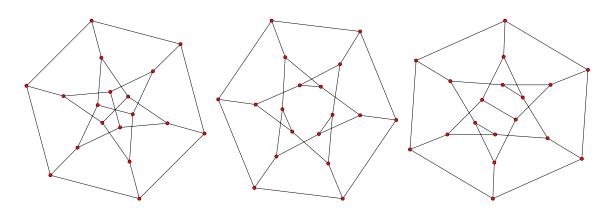
Figure 21: Levi graphs for the three 9_3 configurations. The first one corresponds to the Pappus configuration while the second one is a Haar graph $H(261)$.
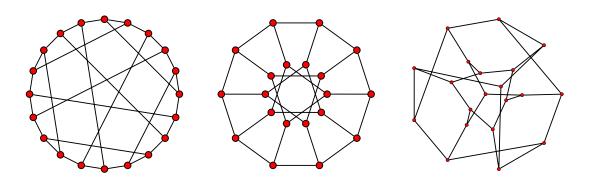

Figure 22: The Levi graph of Desargues configuration. This is the same as $GP(10, 3)$. See also Figure 26.
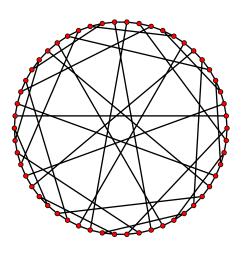
Figure 24: The Gray graph, which is the Levi graph of a flag-transitive non-self-dual 27_3 configuration.

For instance, the Fano configuration cannot be drawn with all lines straight, but not more than one curved line is needed; see Figure 18. A modern version of Theorem 5 can be found in algorithmic form in [6] and has also been implemented as a computer program [57].

Alspach and Zhang [1] proved that every cubic Cayley graph of a dihedral group is Hamiltonian. Compare also [2]. This result covers also cubic Haar graphs. Hence it applies to cyclic configurations.

Proposition 2 (Alspach and Zhang) *A Levi graph of a cyclic n_3 configuration is Hamiltonian.*

One can show that all Levi graphs for cyclic $n_r, r > 2$ configurations have girth 6. In other words, all non-trivial cyclic configurations contain triangles.

It is perhaps of interest to note that there exist flag-transitive, non-self-dual configurations. Figure 24 depicts the Levi graph of one such configuration, known as the Gray configuration of type 27_3. Since it has all flags indistinguishable it must have all points alike and all lines alike. However, if we interchange the role of points and lines we do not get the same configuration.

As we mentioned earlier, the generalized Petersen graph $G(10, 3)$ is the Levi graph of the Desargues configuration. It is interesting that is appears in a different context.

Let us start with the five element set $\{A, B, C, D, E\}$ partitioned into 2-3 element sets,

say $AB\text{-}CDE$. Two partitions are adjacent, if and only if they have disjoint 2-element sets. For instance $AB\text{-}CDE$ is adjacent to $CD\text{-}ABE$, $CE\text{-}ABD$, and $DE\text{-}ABC$. The resulting graph shown in Figure 25 is the Petersen graph.

We may repeat this process but now we label the vertices of a trigonal bipyramid. If we use labels AB for the axial position and CDE for the equatorial position we construct the Petersen graph again. This mechanism also allows for the occurrence of the enantiomers (mirror image). If we want to differentiate the two we obtain $GP(10, 3)$, the Levi graph of the Desargues configuration; see Figure 26.

8   Cages and Covering Graphs

The length of the shortest cycle in a graph G is called the girth of G. For a simple graph the girth is at least 3. The smallest trivalent graph of girth g is called a g-cage. Obviously K_4 is the unique 3-cage and $K_{3,3}$ is the only 4-cage. The Petersen graph is the only 5-cage.

It turns out that the 6-cage is the Heawood graph; see Figure 19. The 7-cage has 24 vertices and is depicted on Figure 30. It was Tutte who proved that the 8-cage is the graph of the Cremona-Richmond configuration. That is why this graph is more often called the Tutte 8-cage.

It is interesting that the 9-cage was not found until quite recently. The search for the 9-cage involved a lot of computer checking and the result came as a surprise. There are 18 non-isomorphic 9-cages. All smaller cages have regular structure and are all unique. However, the 9-cages do not show any apparent structure; they are computed in [10].

Balaban found one of the three 10-cages which is shown in Figure 28. It is perhaps of interest to note that the 10-cages were known before all the 9-cages were computed. The reason is simply in the fact that the gap between easily proven lower bound and the actual size of the cage is larger for the 9-cage than for the 10-cage. One can prove that there is no trivalent graph of girth 9 on 46 or less vertices and that there is no such graph of girth 10 on 62 or less vertices. Since the 9-cage has 58 vertices and the 10-cage has 70 vertices the respective gaps are 12 for the 9-cage and only 8 for the 10-cage. For a survey on cages, see [69].

There is a way of describing certain large graphs using labels on smaller ones. We will introduce this method using the cages as examples.

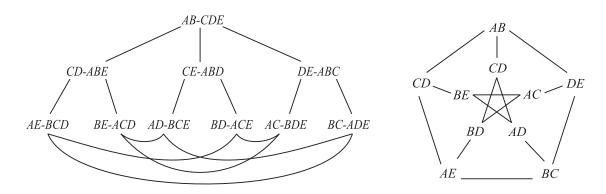Let us start with the *5-cage*, the Petersen graph.
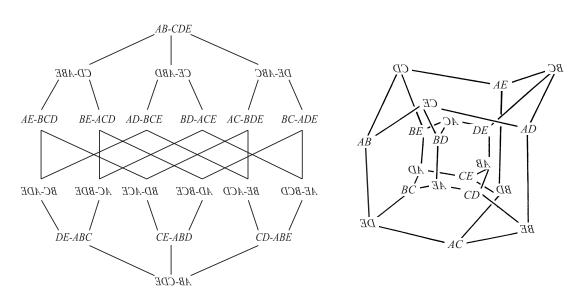
Figure 25: The Petersen graph $GP(5,2)$.

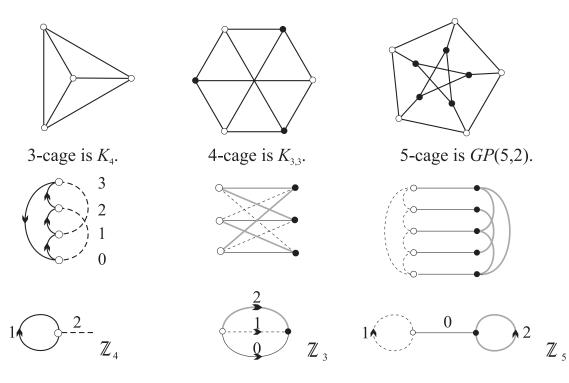Figure 26: $GP(10,3)$ is the Kronecker double cover of $GP(5,2)$.

Figure 27: The 3-, 4- and 5-cages as covering graphs. At the bottom the corresponding voltage graphs are shown.
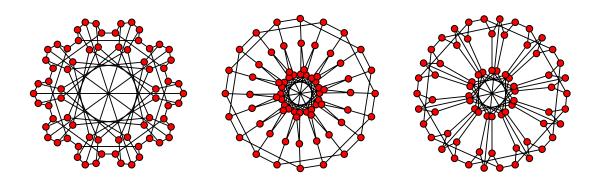

Figure 28: Three views of Balaban's 10-cage.

We will project the Petersen graph onto a hand-cuff graph. The *handcuff graph* is not simple. It has two loops attached to the endpoints of a single edge. The outer circle is projected to one loop, the inner pentagram is projected to the second loop and the rims are projected to the edge between the loops. We may direct the edges of the hand-cuff graph and assign permutations on the edges as shown in the figure . . . The first loop gets permutation $(1, 2, 3, 4, 5)$, the second loop gets $(1, 3, 5, 2, 4)$ and the edge gets the identity $(1)(2)(3)(4)(5)$. The assignment of the permutations on the edges of the handcuff graph is called the *permutation voltage assignment*. Now we will show how to construct the permutation derived graph. Above each vertex of the handcuff graph we place five vertices one on each layer. Above each edge of the handcuff graph we place five edges. However, the edge that was directed from a to b and having voltage p runs from the vertex above a on layer i to the vertex above b on layer $p(i)$. The resulting graph is clearly the Petersen graph. In this case we have a shortcut. Instead of permutations we can assign group elements from Z_5. First loop gets 1, second loop 3 and the edge 0. This is called the *ordinary voltage assignment*.

Now we label the layers by group elements and perform the operation again, getting the same result. The *voltage graph* is also called the *base graph* and the derived graph is called the *covering graph*. The terminology follows the one of covering spaces in algebraic topology. The reader is referred to the book by Gross and Tucker [28] for further information about graph coverings. The Petersen graph obtained in this way can be labeled as $GP(5, 3)$. This means that we are working in the group Z_5 and that the voltage on the second loop is 3. Note that this process can be generalized Petersen graphs $GP(n, k)$ with group Z_n and voltage k.

If the covering graph is trivalent then the base graph must be trivalent as well. It may have loops and parallel edges. Even though we assigned voltages to directed edges, we get the same result if we change the direction at an edge. We only have to assign the inverse voltage to the reversely directed edge. We may also have to allow *halfedges* in the base graph. The only condition is the half-edge must have an involutory voltage.

The *3-cage* is the covering graph over the graph with a single vertex with a loop and a half edge. The voltages are taken in Z_4. The loop gets voltage 1 and the half-edge gets the voltage 2.

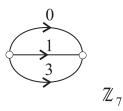The *4-cage* is the 3-fold covering graph over the theta graph (with the voltages 0,1,2 in Z_3.

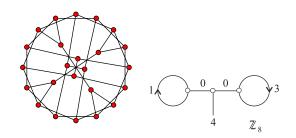Figure 29: The theta graph, equipped with voltages from Z_7 for the 6-cage.

Figure 30: The 7-cage with its voltage graph. This is also known as the McGee graph.

Taking the theta graph and the voltages 0, 1, and 3 in Z_4 we get the graph Q_3, but the same voltages in Z_7 (see Figure 29) define the *6-cage*, i.e. the Heawood graph.

The *7-cage* is an 8-fold covering graph over the voltage graph on 3 vertices; see Figure 30.

The *8-cage* can be represented as a 5-fold covering graph over a graph on 6 vertices; see Figure 31.

We should mention two special constructions. One is called the *Kronecker double cover*. For an arbitrary graph G we may label all the edges with 1, the non-trivial element of the two-element group Z_2. This defines the double cover graph, $G(2)$ also known as the tensor product by K_2. Here are some examples:
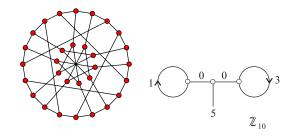

Figure 31: The 8-cage with its voltage graph. This is also known as the Cremona-Richmond graph.

Graph	Kronecker double cover
P_n	$2P_n$
C_{2n}	$2C_{2n}$
C_{2n+1}	C_{4n+2}
K_4	Q_3
G - bipartite	$2G$
$GP(5,2)$	$GP(10,3)$

Recall that $GP(4,1)$ is the cube Q_3. It turns out that $GP(8,3)$, $GP(12,5)$ and $GP(24,5)$ are its covers, [8]. On the other hand, $GP(5,2)$ is the Petersen graph whose canonical (Kronecker) double cover is $GP(10,3)$, as clearly seen on Figures 25 and 26, while $GP(10,2)$, the skeleton of the dodecahedron, arises as a double cover of its pentagonal embedding in the projective plane. An interesting project would be to determine the Kronecker double covers of all generalized Petersen graphs $GP(n,k)$.

The simplest voltage graph G has the voltage group Z_n and has only two types of voltage labels: the trivial 0 and the non-trivial 1. In this case the covering graph is called a *rotagraph*. The subgraph M of G composed of those edges of G with trivial voltages is called a *monograph*; see [56] for more information on rotagraphs.

Many well-known graphs can be described as rotagraphs, for example the prisms and antiprisms. However, the Petersen graph is not a rotagraph although it has a rotational symmetry. In this case we need jumps of size one as well as jumps of size 2. Hence, we will call the covering graph obtained by the cyclic group Z_n a generalized rotagraph. The main idea about generalized rotagraphs is that we may easily keep the voltages and vary n. So we always get not only one graph but an infinite family of graphs of the same type. Viewing the Petersen graph as a generalized rotagraph, we immediately get the whole family $GP(n,2)$.

The notion of cages can be generalized to other regular graphs. A (d,g)-*cage* is the smallest regular d-valent graph with girth g.

In Figures 28,32,33, and 34 are given some known examples, perhaps drawn in a new way.

Recently Markus Meringer showed by computer that there are exactly 4 $(5,5)$-cages. His computer program `genreg`, which can generate all connected k-regular graphs with a given minimum girth, found the fourth $(5,5)$-cage and proved that there are no other ones, [50].

9   Conclusion

Most of the figures in this paper were created by programs that are integrated in the system Vega
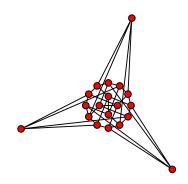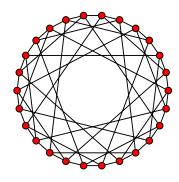

Figure 32: The (4,5)-cage.
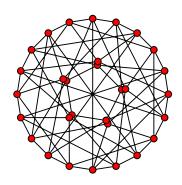

Figure 33: The (4,6)-cage.

Figure 34: The fourth (5,5)-cage.

[57]. For graph drawings, variations of the so-called spring embedder were used.

References

[1] B. Alspach and C. Q. Zhang. Hamilton cycles in cubic Cayley graphs on dihedral groups. *Ars. Combin.*, 28:101–108, 1989.

[2] B. Alspach, C. C. Chen, and K. McAvaney. On a class of Hamilton laceable 3-regular graphs. *Discr. Math.*, 151:19–38, 1996.

[3] Anton Betten and Dieter Betten. Regular Linear Spaces. *Beiträge zur Algebra und Geometrie*, 38:1, 111–124, 1997.

[4] A. Betten, G. Brinkmann, and T. Pisanski. Counting symmetric configurations v_3, submitted.

[5] N. Biggs. *Algebraic Graph Theory*, Second Edition. Cambridge Univ. Press, Cambridge, 1993.

[6] J. Bokowski and B. Strumfels. *Computational Synthetic Geometry*. LNM 1355, Springer-Verlag, 1989.

[7] J. A. Bondy and U. S. R. Murty. *Graph Theory with Applications*. American Elsevier Publishing Co., 1976.

[8] I. Z. Bouwer et al, editors. *The Foster Census*. The Charles Babbage Research Centre, Winnipeg, Canada, 1988.

[9] G. Brinkmann. Fast Generation of Cubic Graphs. *J. Graph Theory*, 23:139–149, 1996.

[10] G. Brinkmann, B. D. McKay, and C. Saager. The smallest cubic graph of girth 9. *Combinatorics, Probability and Computing*, 5:1–13, 1995.

[11] H. S. M. Coxeter. *Regular Polytopes*, Third Edition. Dover Publications Inc., New York, 1973.

[12] H. S. M. Coxeter. Self-dual configurations and regular graphs. *Bull. Amer. Math. Soc.*, 56:413–455, 1950.

[13] H. S. M. Coxeter, R. Frucht, and D. L. Powers. *Zero-Symmetric Graphs*. Academic Press, New York, 1981.

[14] H. S. M. Coxeter and W. O. J. Moser. *Generators and Relators for Discrete Groups*, Fourth Edition. Springer-Verlag, 1980.

[15] H. M. Cundy and A. R. Rollett. *Mathematical Models*, Third Edition. Tarquin Publications, Norfolk, 1981.

[16] R. Daublebsky von Sterneck. Die Configurationen 11_3. *Monatsh. Math. Physik*, 5:325–330, 1894.

[17] R. Daublebsky von Sterneck. Die Configurationen 12_3. *Monatsh. Math. Physik*, 6:223–255, 1895.

[18] P. Dembowski. *Finite Geometries*. Ergebnisse der Mathematik und ihre Greenzgebiete, Bd. 44, Springer-Verlag, New York, 1968.

[19] S. F. Du, D. Marušič, and A. O. Waller. On 2-arc-transitive covers of complete graphs, submitted.

[20] P. Fowler and T. Pisanski. Leapfrog Transformation and Polyhedra of Clar Type. *J. Chem. Soc. Faraday Trans.*, 90:2865–2871, 1994.

[21] R. Frucht, J. E. Graver, and M. E. Watkins. The groups of the generalized Petersen graphs. *Proc. Cambridge Philos. Soc.*, 70:211–218, 1971.

[22] M. C. Golumbic. *Algorithmic Graph Theory and Perfect Graphs*. Academic Press, New York 1980.

[23] H. Gropp. On the history of configurations. In A. Deza, J. Echeverria and A. Ibarra, editors, *Internat. Symposium on Structures in Math. Theories*, pages 263–268, Bilbao, 1990.

[24] H. Gropp. Configurations and Graphs. *Discrete Math.*, 111:269–276, 1993.

[25] H. Gropp. The Construction of All Configurations $(12_4, 16_3)$. In J. Nešetřil and M. Fiedler, editors, *Fourth Czechoslovak Symposium on Combinatorics, Graphs and Complexity*, pages 85–91, Elsevier, 1992.

[26] H. Gropp. Configurations and their realizations. *Discrete Math.* 174:137–151, 1997.

[27] H. Gropp. Configurations. In C. J. Colburn and J. H. Dinitz, editors, *The CRC Handbook of Combinatorial Designs*, 253–255, CRC Press, 1996.

[28] J. L. Gross and T. W. Tucker. *Topological Graph Theory.* Wiley Interscience, 1987.

[29] L. Grossman and W. Magnus. *Groups and their graphs.* Random House, New York, 1966.

[30] T. F. Havel. The Combinatorial Distance Geometry Approach to the Calculation of Molecular Conformation, Ph. D. Thesis (Biophysics), Berkeley, 1982.

[31] N. Hartsfield and G. Ringel. *Pearls in Graph Theory*, Revised Edition. Academic Press, New York, 1994.

[32] D. Hilbert and S. Cohn-Vossen. *Geometry and the Imagination.* Chelsea Publishing Co., New York, 1952.

[33] M. Hladnik and T. Pisanski. Schur Norms of Haar Graphs, work in progress.

[34] M. Hladnik, D. Marušič, and T. Pisanski. Haar graphs, work in progress.

[35] D. A. Holton and J. Sheehan. *The Petersen Graph.* Cambridge Univ. Press, 1993.

[36] H. Hosoya, Y. Okuma, Y. Tsukano, and K. Nakada. Multilayered Cyclic Fence Graphs: Novel Cubic Graphs Related to the Graphite Network. *J. Chem. Inf. Comp. Sci.*, 35:351–356, 1995.

[37] A. Jurišić. Antipodal Covers, Ph.D. Thesis, University of Waterloo, Canada, 1995.

[38] M. Kaufman, T. Pisanski, D. Lukman, B. Borštnik, and A. Graovac. Graph-drawing algorithms geometries versus molecular mechanics in fullerenes. *Chem. Phys. Letters*, 259:420–424, 1996.

[39] S. Klavžar and M. Petkovšek. Intersection graphs of halflines and halfplanes. *Discrete Math.*, 66:133–137, 1987.

[40] D. J. Klein. Graph geometry, graph metrics, and Wiener. *MATCH*, 35:7–27, 1997.

[41] D. J. Klein, M. Randić. Resistance Distance. *J. Math. Chemistry*, 12:81–95, 1993.

[42] D. J. Klein, H. Zhu. All-Conjugated Carbon Species. In A. T. Balaban, editor, *From Chemical Topology to Three-Dimensional Geometry*, pages 297–341, Plenum Press, New York, 1997.

[43] M. Lovrečič-Saražin. A note on the generalized Petersen graphs that are also Cayley graphs. *J. Combin. Theory (B)*, 69: 226–229, 1997.

[44] M. Lovrečič-Saražin. Cayleyevi in Petersenovi grafi. *Obzornik Mat. fiz.*, 42:193–198, 1995.

[45] D. Marušič and T. Pisanski. The remarkable generalized Petersen graph $G(8,3)$, submitted.

[46] H. Maehara. Space graphs and sphericity. *Discrete Appl. Math.*, 7:55–64, 1984.

[47] H. Maehara. On the sphericity for the join of many graphs. *Discrete Math.*, 49:311–313, 1984.

[48] H. Maehara. On the sphericity of semiregular polyhedra. *Discrete Math.*, 58:311–315, 1986.

[49] R. E. Maeder. Uniform Polyhedra. *The Mathematica Journal*, 3(4):48–57, 1993.

[50] M. Meringer. Computer Program `genreg`, `ftp://132.180.16.20`

[51] M. Meringer: Erzeugung regulärer Graphen, Master's thesis, Universität Bayreuth, January 1996.

[52] S. Negami. Diagonal Flips in Triangulations of Surfaces. *Discr. Math.*, 135:225–232, 1994.

[53] T. Pisanski, B. Plestenjak, and A. Graovac. NiceGraph Program and its application in Chemistry. *Croatica Chemica Acta*, 68:283–292, 1995.

[54] T. Pisanski, B. Plestenjak, and A. Graovac. Generating Fullerenes at Random. *J. Chem. Inf. Comp. Sci.*, 36:825–828, 1996.

[55] T. Pisanski, M. Razinger, and A. Graovac. Geometry versus Topology: Testing Self-consistency of the NiceGraph Program. *Croatica Chemica Acta*, 69 (in press), 1996.

[56] T. Pisanski, A. Žitnik, A. Graovac, and A. Baumgartner. Rotagraphs and their generalizations. *J. Chem. Inf. Comp. Sci.*, 34:1090–1093, 1994.

[57] T. Pisanski, editor. *Vega Version 0.2; Quick Reference Manual and Vega Graph Gallery.* IMFM, Ljubljana, 1995. `http://vega.ijp.si/`

[58] M. Randić. Symmetry Properties of graphs of Interest in Chemistry. II. Desargues - Levi Graph. *Int. J. Quant. Chem.*, 15:663–682, 1979.

[59] G. Ringel. *Map Color Theorem.* Springer-Verlag, Berlin, 1974.

[60] F. S. Roberts. Indifference graphs. In F. Harary, editor, *Proof Techniques in graph theory*, pages 139–146, Academic Press, 1969.

[61] R. Sayle. RasMol V2.5, `http://www.bio.cam.ac.uk/doc/rasmol.html`

[62] E. Steinitz. *Über die Construction der Configurationen n_3.* Dissertation, Breslau, 1894.

[63] E. Steinitz (with H. Rademacher). *Vorlesungen über die Theorie der Polyeder.* Springer-Verlag, Berlin, 1934.

[64] B. Sturmfels and N. White. All 11_3 and 12_3 configurations are rational. *Aequationes Mathematicae*, 39:254–260, 1990.

[65] T. W. Tucker. There is only one group of genus two. *J. Combin. Theory B*, 36:269–275, 1984.

[66] D. Wells. *The Penguin Dictionary of Curious and Interesting Geometry.* Penguin Books, London, 1991.

[67] A. White. *Graphs, Groups, and Surfaces.* North-Holland Pub. Co., Amsterdam, 1973.

[68] R. Wilson. *Introduction to Graph Theory.* Academic Press, New York, 1979.

[69] P. K. Wong. Cages — a survey. *J. Graph Theory*, 6:1–22, 1982.